

## Heavy-Metal Aromatic and Conjugated Species: Rings, Oligomers, and Chains of Tin in $\text{Li}_{9-x}\text{EuSn}_{6+x}$ , $\text{Li}_{9-x}\text{CaSn}_{6+x}$ , $\text{Li}_5\text{Ca}_7\text{Sn}_{11}$ , $\text{Li}_6\text{Eu}_5\text{Sn}_9$ , $\text{LiMgEu}_2\text{Sn}_3$ , and $\text{LiMgSr}_2\text{Sn}_3$

Iliya Todorov and Slavi C. Sevov\*

Department of Chemistry and Biochemistry, University of Notre Dame, Notre Dame, Indiana 46556

Received May 18, 2005

The title compounds were synthesized from the elements by heating the corresponding mixtures at high temperature. Their structures were determined from single-crystal X-ray diffraction.  $\text{Li}_{9-x}\text{EuSn}_{6+x}$ ,  $\text{Li}_{9-x}\text{CaSn}_{6+x}$ ,  $\text{Li}_5\text{Ca}_7\text{Sn}_{11}$ , and  $\text{Li}_6\text{Eu}_5\text{Sn}_9$  contain columns of stacked aromatic pentagons of  $\text{Sn}_5^{6-}$  that are analogous to the cyclopentadienyl anion  $\text{C}_5\text{H}_5^-$ . The pentagons are separated with  $\text{Ca}^{2+}$  or  $\text{Eu}^{2+}$  in the columns and resemble a polymeric metallocene. In addition to the columns, the isostructural  $\text{Li}_{9-x}\text{EuSn}_{6+x}$  and  $\text{Li}_{9-x}\text{CaSn}_{6+x}$  contain isolated tin atoms and bent tin trimers while  $\text{Li}_5\text{Ca}_7\text{Sn}_{11}$  and  $\text{Li}_6\text{Eu}_5\text{Sn}_9$  contain flat zigzag hexamers and flat zigzag infinite chains of tin, respectively. The isostructural  $\text{LiMgEu}_2\text{Sn}_3$  and  $\text{LiMgSr}_2\text{Sn}_3$  do not contain columns of pentagons but only flat zigzag infinite chains of tin. The aromaticity of the pentagons and the conjugation of the  $\pi$ -systems of the hexamers and the infinite chains are discussed. The title compounds are also characterized by magnetic and conductivity measurements.

### Introduction

One of the most fascinating and structurally diverse classes of solid-state compounds are the polar intermetallics, i.e., intermetallics made of the very electropositive alkali, alkaline-earth, and/or rare-earth metals and the relatively more electronegative *p*-block metals. Due to the large differences in electronegativities, these compounds, known as Zintl phases, are viewed as salts resulting from complete electron transfer from the less to the more electronegative constituent. Typically, the resulting cations are treated simply as closed-shell point charges that (a) keep the anions together through electrostatic forces and (b) occupy space that, when appropriate in size, provides for efficient packing with the anions in a crystalline structure. The exciting feature in such an intermetallic compound is rather the anionic part with its structure, bonding, electronic structure, potential for excision and eventual stability in solutions, etc. The structural diversity of this anionic part is indeed vast and correlates quite well with the level of reduction of the post-transition metal. Thus, the structures span from three-dimensional frameworks that resemble the elemental structures of the *p*-elements (at low reduction levels) to lower dimension formations such as

layers, chains, and clusters as more and more of the electropositive element is added.

One particular system that we have studied extensively and very systematically is that of alkali metal (A)/alkaline-(or rare)-earth metal (Ae,Re)/tin. Our results and those of others clearly indicate that the heavier alkali metals Na, K, Rb, and Cs, act exactly as simple electron donors with different sizes as discussed above. Thus, the corresponding structures are defined almost exclusively by the degree of reduction of tin and can be viewed as being generated from elemental tin upon breaking more and more bonds. Some of the compounds produced upon such successive reduction are as follows (given in parentheses is the number of positive charges per tin atom for each compound): the less-reduced  $\text{A}_8\text{Sn}_{44}$  (0.182),<sup>1</sup>  $\text{ASn}_5$  (0.200),<sup>2</sup>  $\text{A}_{32.7}\text{Sn}_{162.4}$  (0.202),<sup>3</sup>  $\text{A}_{8-x}\text{Sn}_{25}$  ( $\leq 0.320$ ),<sup>1c</sup> and  $\text{A}_5\text{Sn}_{13}$  (0.385)<sup>4</sup> with three-dimensional anionic frameworks, the more reduced  $\text{A}_{24}\text{Sn}_{36}$  (0.667)<sup>5</sup> with clathrate-like layers and isolated  $\text{Sn}_4^{4-}$  tetrahedra and  $\text{A}_4$ -

- (1) (a) Gallmeier, J.; Schafer, H.; Weiss, H. *Z. Naturforsch.* **1969**, *24b*, 665. (b) Grin, Y.; Melekhov, L. Z.; Chuntunov, L. Z.; Yatsenko, S. P. *Sov. Phys. Crystallogr.* **1987**, *32*, 290. (c) Zhao, J. T.; Corbett, J. D. *Inorg. Chem.* **1994**, *33*, 5721.
- (2) Kronseder, C.; Fessler, T. *Angew. Chem., Int. Ed. Engl.* **1998**, *37*, 1571.
- (3) Bobev, S.; Sevov, S. C. *J. Am. Chem. Soc.* **2001**, *123*, 3389.
- (4) Vaughney, J. T.; Corbett, J. D. *Inorg. Chem.* **1997**, *36*, 4316.
- (5) Bobev, S.; Sevov, S. C. *Inorg. Chem.* **2000**, *39*, 5930.

\* To whom correspondence should be addressed. E-mail: ssevov@nd.edu.

$\text{Sn}_9$  (0.444)<sup>6</sup> and  $\text{A}_{12}\text{Sn}_{17}$  (0.706)<sup>7</sup> with isolated nine-atom clusters of  $\text{Sn}_9^{4-}$  ( $\text{A}_{12}\text{Sn}_{17}$  contains also  $\text{Sn}_4^{4-}$ ), and finally  $\text{A}_4\text{Sn}_4$  (1.000)<sup>8</sup> with  $\text{Sn}_4^{4-}$  tetrahedra where the formal negative charge of each tin atom is  $-1$  (a three-bonded tin atom). The picture becomes much more interesting when more covalent electropositive elements such as Li, Ae, and/or Re are added to the system. These cations have a much stronger preference for specific coordination with the anions.<sup>9–12</sup> Thus, addition of Li to the Rb/Sn system stabilizes square antiprisms of  $\text{Sn}_8^{6-}$  in  $\text{Rb}_4\text{Li}_2\text{Sn}_8$  (0.750) with lithium capping the two open square faces of the antiprisms and, in addition, interacting with the edges of neighboring prisms (the lone pairs of electrons at the tin atoms).<sup>10</sup> Similarly, four Ba cations center four pentagonal dodecahedra fused together in a huge isolated cluster of 56 tin atoms,  $[\text{Ba}_4@\text{Sn}_{56}]^{36-}$  in  $\text{Na}_{204}\text{Ba}_{16}\text{Sn}_{310}$  (0.761).<sup>11</sup> Clearly, the driving force for the formation of such remarkable species is the need for barium to be spherically saturated (coordinated) with anionic tin. Note the small amount of barium with respect to the alkali metal in this compound, almost at doping level (four out of 55 cations), but its presence causes formation of a completely new structural motif. Of course, addition of alkaline-earth (“dilution” of the alkali metal) favors structures with more reduced tin simply because of the higher charge of the cations. Thus, further addition of Ae, Ca, or Sr in this case leads to  $\text{Na}_{10}\text{AeSn}_{12}$  (1.000) with truncated tetrahedra of  $\text{Sn}_{12}^{12-}$  (all three-bonded tin atoms) centered by the alkali-earth cations.<sup>12</sup> We point out that the formal negative charge of tin in this compound is exactly the same as in  $\text{A}_4\text{Sn}_4$  ( $\text{A} = \text{Na}, \text{K}, \text{Rb}, \text{Cs}$ ), which contains simple  $\text{Sn}_4^{4-}$  tetrahedra.<sup>8</sup> Therefore, the reason for the formation of  $\text{Sn}_{12}^{12-}$  in  $\text{Na}_{10}\text{AeSn}_{12}$  must be the greater covalency of Ca and Sr compared to Na, K, Rb, and Cs and a resulting stronger tendency to coordinate with tin atoms.<sup>12</sup>

Further increase of the number of positive charges per tin atom combined with an increased fraction of alkaline-earth cations would make the tin atoms formally more negative than  $-1$  on average. This was realized in the isostructural compounds  $\text{Na}_8\text{BaSn}_6$  and  $\text{Na}_8\text{EuSn}_6$  (and the lead analogue  $\text{Na}_8\text{BaPb}_6$ ) with 1.667 positive charges per tin atom, i.e., formal average negative charge of  $-1.667$  per tin.<sup>13</sup> We point out that the formal charge of an individual tin atom depends on the number of bonds to this atom. Thus, 4-, 3-, 2-, 1-, and 0-bonded tin atoms (2-center-2-electron bonds) correspond to  $\text{Sn}^0$ ,  $\text{Sn}^-$ ,  $\text{Sn}^{2-}$ ,  $\text{Sn}^{3-}$ , and  $\text{Sn}^{4-}$ , respectively. Therefore, the average number of bonds to a tin atom with an average charge of  $-1.667$  is expected to be between 2 and 3. However, in  $\text{Na}_8\text{AeSn}_6$  this charge is achieved differently; one of the six tin atoms is isolated, i.e., 0-bonded  $\text{Sn}^{4-}$ , while the remaining five atoms form a flat ring of

$\text{Sn}_5^{6-}$ . The latter is isostructural and isoelectronic with the aromatic cyclopentadienyl anion  $\text{C}_5\text{H}_5^-$  and must be viewed as aromatic as well (also  $\text{Pb}_5^{6-}$  in  $\text{Na}_8\text{BaPb}_6$  and  $\text{Si}_5^{6-}$  in  $\text{Li}_8\text{MgSi}_6^{14}$ ). These pentagonal rings of tin and lead are the heaviest aromatic species known so far. The rings are stacked on top of each other in these structures, and the alkaline- or rare-earth cations are found between the rings in the stacks. Again, the structures are possible because of the stronger tendency of the Ae and Re cations to coordinate to anions, in this case to the aromatic systems of  $\text{Sn}_5^{6-}$  forming infinite metallocene-like columns.

We have expanded our methodical exploration of these systems by changing the alkali metal to the much more covalent lithium and by further increasing the fraction of alkaline- or rare-earth cations. We find that the columns of stacked pentagonal rings are apparently very stable formations that are found in more compounds where they coexist with various other motifs. Here, we report the structures and properties of  $\text{Li}_{9-x}\text{EuSn}_{6+x}$ ,  $\text{Li}_{9-x}\text{CaSn}_{6+x}$ ,  $\text{Li}_5\text{Ca}_7\text{Sn}_{11}$ , and  $\text{Li}_6\text{Eu}_5\text{Sn}_9$  with such columns and of  $\text{LiMgEu}_2\text{Sn}_3$ ,  $\text{LiMgSr}_2\text{Sn}_3$  with only conjugated chains. In addition to the columns, compounds  $\text{Li}_{9-x}\text{EuSn}_{6+x}$  and  $\text{Li}_{9-x}\text{CaSn}_{6+x}$  contain isolated tin atoms and bent trimers,  $\text{Li}_5\text{Ca}_7\text{Sn}_{11}$  has flat hexamers, and  $\text{Li}_6\text{Eu}_5\text{Sn}_9$  contains also flat infinite zigzag chain of tin. The lithium atoms in all these compounds not only provide electrons and fill space between the anions but also interact covalently, i.e., through directional interactions, with the tin anions by coordinating to their available lone-pairs of electrons. The positioning of lithium with respect to the tin atoms in some of these motifs resembles that of protons with respect to carbon in hydrocarbons with conjugated  $\pi$ -systems.

## Experimental Section

**Synthesis.** All manipulations were carried out in an argon-filled glovebox with a moisture level below 1 ppm (vol). The starting materials Li (granular, 99+%), Mg (turnings, Alfa, 99.8%), Ca or Sr (granules, Strem, 99.5%), and Sn (rod, Alfa, 99.999%) were used as received, while the surface of Eu (ingot, Ames Laboratory DOE, 99.9%) was removed with a scalpel before use. In a typical synthesis, a mixture of the elements was placed in a niobium tube that was then sealed by arc-welding. The tube was in turn jacketed in a silica ampule that was then flame-sealed under vacuum. All title compounds are highly air- and moisture-sensitive.

Initially, the compounds were discovered as minor products from exploratory reactions loaded with various ratios between the elements. The reactions were heated at 860 °C for 1 week and were then cooled to room temperature with a rate of 1 °C/min. Some other products of these reactions were (a) the known  $\text{Li}_7\text{Sn}_3$ ,  $\text{MgSrSn}$ , and  $\text{EuSn}$ , (b)  $\text{Eu}_3\text{Sn}_5$  and  $\text{LiRb}_7\text{Sn}_8$  isostructural with  $\text{Ae}_3\text{Sn}_5$  and  $\text{LiCs}_7\text{Ge}_8$ , respectively, and (c)  $\text{Eu}_4\text{Sn}_3$  with a novel structure. After the stoichiometries of the title compounds were determined from single-crystal X-ray diffraction, they were synthesized as single-phase products from the corresponding stoichiometric mixtures of the elements treated at the same temperature regime. The samples for property measurements were made by quenching of the reactions from 860 °C in liquid nitrogen. The purity of the compounds was confirmed by powder X-ray diffraction

(6) Hoch, C.; Wendorff, M.; Rohr, C. *Acta Crystallogr.* **2002**, C58, 45.

(7) Hoch, C.; Wendorff, M.; Rohr, C. *J. Alloys Compd.* **2003**, 361, 206.

(8) (a) Muller, W.; Volk, K. *Z. Naturforsch.* **1977**, 32b, 709. (b) Hewaidy, I. F.; Busmann, E.; Klemm, W. *Z. Anorg. Allg. Chem.* **1964**, 328, 283.

(9) Nesper, R. *Prog. Solid State Chem.* **1990**, 20, 1.

(10) Bobev, S.; Sevov, S. C. *Angew. Chem., Int. Ed.* **2000**, 39, 4108.

(11) Bobev, S.; Sevov, S. C. *J. Am. Chem. Soc.* **2002**, 124, 3359.

(12) Bobev, S.; Sevov, S. C. *Inorg. Chem.* **2001**, 40, 5361.

(13) Todorov, I.; Sevov, S. C. *Inorg. Chem.* **2004**, 43, 6490.

(14) Nesper, R.; Curda, J.; v. Schnering, H. G. *J. Solid State Chem.* **1986**, 62, 199.

**Table 1.** Selected Data Collection and Refinement Parameters for  $\text{Li}_{9-x}\text{EuSn}_{6+x}$ ,  $\text{Li}_{9-x}\text{CaSn}_{6+x}$ ,  $\text{Li}_6\text{Eu}_5\text{Sn}_9$ ,  $\text{Li}_5\text{Ca}_7\text{Sn}_{11}$ ,  $\text{LiMgEu}_2\text{Sn}_3$ , and  $\text{LiMgSr}_2\text{Sn}_3$ 

chemical formula	$\text{Li}_{9-x}\text{EuSn}_{6+x}$	$\text{Li}_{9-x}\text{CaSn}_{6+x}$	$\text{Li}_6\text{Eu}_5\text{Sn}_9$	$\text{Li}_5\text{Ca}_7\text{Sn}_{11}$	$\text{LiMgEu}_2\text{Sn}_3$	$\text{LiMgSr}_2\text{Sn}_3$
fw	958.79	846.91	1869.65	1620.85	691.24	562.56
space group, Z	<i>Cmcm</i> , 4	<i>Cmcm</i> , 4	<i>Cmcm</i> , 4	<i>Cmcm</i> , 4	<i>Cmcm</i> , 4	<i>Cmcm</i> , 4
<i>a</i> (Å)	4.723(1)	4.640(1)	4.827 (1)	4.666(1)	4.782(1)	4.843(1)
<i>b</i> (Å)	27.125(1)	27.111(1)	28.948(1)	20.717(2)	20.717(1)	20.922(1)
<i>c</i> (Å)	11.435(1)	11.490(1)	15.006(1)	31.619(6)	7.742(1)	7.804(1)
<i>V</i> (Å <sup>3</sup> )	1465.1(3)	1445.5(3)	2097.0(5)	2517.1(6)	769.7(1)	790.9(2)
radiation, $\lambda$ (Å)	Mo K $\alpha$ , 0.710 73	Mo K $\alpha$ , 0.710 73	Mo K $\alpha$ , 0.710 73	Mo K $\alpha$ , 0.710 73	Mo K $\alpha$ , 0.710 73	Mo K $\alpha$ , 0.710 73
$\rho_{\text{calc}}$ (g·cm <sup>-3</sup> )	4.349	3.826	5.922	4.277	5.985	4.725
$\mu$ (cm <sup>-1</sup> )	147.0	107.7	251.7	121.1	257.0	227.0
R1/wR2, <sup>a</sup> $I \geq 2\sigma_1$ (%)	4.49/10.99	3.28/8.23	2.97/6.21	3.65/8.01	2.66/7.25	8.22/19.18
R1/wR2, <sup>a</sup> all data (%)	5.08/11.29	3.84/8.68	4.40/6.70	6.57/9.09	2.79/7.33	8.59/19.75

$$^a \text{R1} = [\sum||F_o| - |F_c||]/\sum|F_o|; \text{wR2} = \{[\sum w[(F_o)^2 - (F_c)^2]^2]/[\sum w(F_o)^2]\}^{1/2}; w = [\sigma^2(F_o)^2 + (AP)^2 + BP]^{-1}, \text{ where } P = [(F_o)^2 + 2(F_c)^2]/3.$$

on an Enraf-Nonius Guinier camera under vacuum (Cu K $\alpha$  radiation,  $\lambda = 1.540\ 562$  Å).

**Structure Determination.** Gray to black bar-like or octahedral crystals with metallic luster were selected from each compound and were mounted in thin-walled glass capillaries that were subsequently flame-sealed at both ends. The crystals were checked for singularity on an Enraf-Nonius CAD4 diffractometer with graphite monochromated Mo K $\alpha$  radiation ( $\lambda = 0.710\ 73$  Å). X-ray diffraction data sets were collected at room temperature for the best ones ( $\text{Li}_{9-x}\text{EuSn}_{6+x}$ :  $0.14 \times 0.12 \times 0.12$  mm,  $\text{Li}_{9-x}\text{CaSn}_{6+x}$ :  $0.14 \times 0.1 \times 0.06$  mm,  $\text{Li}_6\text{Eu}_5\text{Sn}_9$ :  $0.22 \times 0.06 \times 0.04$  mm,  $\text{Li}_5\text{Ca}_7\text{Sn}_{11}$ :  $0.2 \times 0.06 \times 0.02$  mm,  $\text{LiMgEu}_2\text{Sn}_3$ :  $0.2 \times 0.08 \times 0.04$  mm,  $\text{LiMgSr}_2\text{Sn}_3$ :  $0.2 \times 0.12 \times 0.05$  mm). The raw data (an octant of a sphere for each structure,  $\omega - 2\theta$  scans,  $\theta_{\text{max}} = 25^\circ$ ) were corrected for absorption with the aid of the average of 3  $\psi$ -scans for  $\text{Li}_6\text{Eu}_5\text{Sn}_9$  and 2  $\psi$ -scans for  $\text{Li}_{9-x}\text{EuSn}_{6+x}$ ,  $\text{Li}_{9-x}\text{CaSn}_{6+x}$ ,  $\text{Li}_5\text{Ca}_7\text{Sn}_{11}$ , and  $\text{LiMgEu}_2\text{Sn}_3$ , while no appropriate reflection could be found for  $\text{LiMgSr}_2\text{Sn}_3$ . The observed extinction conditions and intensity statistics suggested the centrosymmetric space group *Cmcm* for all six compounds. Accordingly, the structures were solved and refined in this space group with the aid of the SHELXTL-V5.1 software package.<sup>15</sup> Further details for the data collections and structure refinements are given in Table 1, while important distances and angles are provided as Supporting Information.

The refinement of  $\text{LiMgEu}_2\text{Sn}_3$  and  $\text{LiMgSr}_2\text{Sn}_3$  revealed that one of the cationic positions is lighter for magnesium but heavier for lithium. Therefore, it was refined with mixed Li/Mg occupancy resulting in Li/Mg atomic fractions of 0.46/0.54 and 0.36/0.64 for  $\text{LiMgEu}_2\text{Sn}_3$  and  $\text{LiMgSr}_2\text{Sn}_3$ , respectively. The exact refined formulas for the two compounds are  $\text{Li}_{0.90(2)}\text{Mg}_{1.10(2)}\text{Eu}_2\text{Sn}_3$  and  $\text{Li}_{0.75(3)}\text{Mg}_{1.25(3)}\text{Sr}_2\text{Sn}_3$ , but they are referred to as  $\text{LiMgEu}_2\text{Sn}_3$  and  $\text{LiMgSr}_2\text{Sn}_3$  throughout the text.

Similarly, one tin position, Sn5, in  $\text{Li}_{9-x}\text{EuSn}_{6+x}$  and  $\text{Li}_{9-x}\text{CaSn}_{6+x}$  refined with partial occupancy, 0.32(1) and 0.21(1)% for  $\text{Li}_{9-x}\text{EuSn}_{6+x}$  and  $\text{Li}_{9-x}\text{CaSn}_{6+x}$ , respectively (see also the Results and Discussion). The remaining fraction to full occupancy was given to lithium. Thus, the formulas of the compounds were refined as  $\text{Li}_{8.71(1)}\text{EuSn}_{6.29(1)}$  and  $\text{Li}_{8.84(1)}\text{CaSn}_{6.16(1)}$ , but they are referred to as  $\text{Li}_{9-x}\text{EuSn}_{6+x}$  and  $\text{Li}_{9-x}\text{CaSn}_{6+x}$  throughout the text.

**Magnetic Measurements.** The magnetizations of  $\text{Li}_{9-x}\text{EuSn}_{6+x}$ ,  $\text{Li}_6\text{Eu}_5\text{Sn}_9$ , and  $\text{LiMgEu}_2\text{Sn}_3$  were measured on a Quantum Design MPMS SQUID magnetometer at a field of 3 T over a temperature range of 10–250 K. In addition, measurements at lower temperatures, down to 2 K, and lower magnetic field, 500 G, were carried out both in zero field cooled (ZFC) and field cooled (FC) modes. Each sample was sealed in a quartz tube between two quartz rods that fit tightly in the tube. The data were corrected for the holder

and for ion-core diamagnetism. The compounds showed Curie–Weiss paramagnetism above 30 K for  $\text{Li}_{9-x}\text{EuSn}_{6+x}$  and  $\text{Li}_6\text{Eu}_5\text{Sn}_9$  and above 10 K for  $\text{LiMgEu}_2\text{Sn}_3$ . These data were fitted with  $\chi_m = C/(T - \Theta)$  with accuracies of the fits better than 99.9%. The following parameters were derived from these fits:  $\mu_{\text{eff}} = 7.85$ , 17.68, and 10.26  $\mu_B$  and  $\Theta = -27.1$ , 12.4, and  $-18.7(1)$  K for  $\text{Li}_{9-x}\text{EuSn}_{6+x}$ ,  $\text{Li}_6\text{Eu}_5\text{Sn}_9$ , and  $\text{LiMgEu}_2\text{Sn}_3$ , respectively. Magnetic transitions were observed for  $\text{Li}_{9-x}\text{EuSn}_{6+x}$  and  $\text{Li}_6\text{Eu}_5\text{Sn}_9$  at low temperatures. No superconductivity was observed.

**Resistivity Measurements.** The electrical resistivities of all compounds were measured by the four-probe method (in-line head from JANDEL with 1 mm spacing) on pressed pellets (2000 psi, 0.11 to 0.16 mm diameter, 1.1 mm thick) over the 224–294 K temperature range inside the cold well of a drybox. Measured was the drop of voltage across the samples at constant currents. Due to the apparent high conductivity of the compounds, the maximum possible current of 10 mA available from the JANDEL RM2 unit was used. Despite this, however, the voltage that was measured was still nearly 0, between 0.02 and 0.03 mV, and its variation with the temperature was out of the range of the measuring unit. Thus, using these measured values, the resistivities of all samples are calculated to be around  $0.14 \times 10^{-5}$   $\Omega\cdot\text{cm}$  and indicate highly conducting compounds. For comparison, the resistivity of elemental Sn is  $0.00917 \times 10^{-5}$   $\Omega\cdot\text{cm}$ .

**Electronic Structure Calculations.** Single-point DFT calculations were carried out on the observed flat pentagonal ring and the flat zigzag oligomer of six tin atoms in  $\text{Li}_5\text{Ca}_7\text{Sn}_{11}$ . The Becke three-parameter density functional with the Lee–Yang–Parr correlation functional (B3LYP) was used in the calculations in conjunction with the 3-21G basis set.<sup>16</sup> The calculations were performed with the Gaussian-98 package, revision A.11.3.<sup>17</sup> Orbital pictures were plotted with Molden.<sup>18</sup> Calculated HOMO–LUMO gaps were 2.25 and 1.26 eV for  $\text{Sn}_5^{6-}$  and  $\text{Sn}_6^{12-}$ , respectively. Extended-Hückel calculations were carried out for the infinite chains of  $\text{Li}_6\text{Eu}_5\text{Sn}_9$  and  $\text{LiMgEu}_2\text{Sn}_3$  ( $H_{ii}$  and  $\zeta_1$  for Sn: 5s,  $-216.16$  eV and 2.12; 5p,  $-28.32$  eV and 1.82) with 468 and 430 *k*-points, respectively.<sup>19</sup>

## Results and Discussion

On average, the tin atoms in the new compounds are formally more reduced than in the reported  $\text{Na}_8(\text{Ba}/\text{Eu})\text{Sn}_6$  (1.667 positive charges per tin atom)<sup>13</sup> and can be ordered in increasing degree of reduction as follows:  $\text{Li}_{9-x}(\text{Eu}/\text{Ca})$ -

(16) (a) Becke, A. D. *Phys. Rev.* **1988**, *38*, 3098. (b) Lee, C.; Yang, W.; Parr, R. G. *Phys. Rev. B* **1988**, *B37*, 785.

(17) Frisch, M. J. et al. *Gaussian 98*, Revision A.11.3; Gaussian, Inc.: Pittsburgh, PA, 2002.

(18) Schaftenaar, G.; Noordik, J. H. *J. Comput.-Aided Mol. Design* **2000**, *14*, 123.

(19) Hoffmann, R. J. *J. Chem. Phys.* **1963**, *39*, 1397.

(15) Bruker Analytical Systems, Madison, WI, 1997.

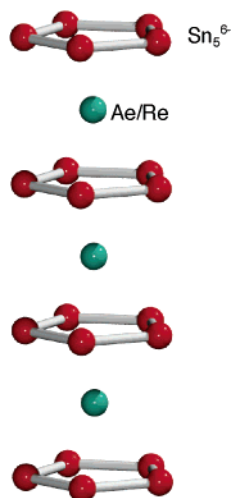


**Figure 1.** Column of eclipsed aromatic pentagons  $\text{Sn}_5^{6-}$  separated by Ae or Re cations found in  $\text{Li}_{9-x}\text{EuSn}_{6+x}$ ,  $\text{Li}_{9-x}\text{CaSn}_{6+x}$ ,  $\text{Li}_5\text{Ca}_7\text{Sn}_{11}$ , and  $\text{Li}_6\text{Eu}_5\text{Sn}_9$ . The distances between the rings (same as the distances between the cations) in the four compounds are 4.645(1), 4.734(1), 4.680(3), and 4.829(1) Å, respectively. The average Ae/Re–Sn distances are 3.401, 3.398, 3.395, and 3.458 Å, respectively.

$\text{Sn}_{6+x}$  (ca. 1.686),  $\text{Li}_5\text{Ca}_7\text{Sn}_{11}$  (1.727),  $\text{Li}_6\text{Eu}_5\text{Sn}_9$  (1.778), and  $\text{LiMg}(\text{Eu}/\text{Sr})_2\text{Sn}_3$  (2.333). The first three structures,  $\text{Li}_{9-x}(\text{Eu}/\text{Ca})\text{Sn}_{6+x}$ ,  $\text{Li}_5\text{Ca}_7\text{Sn}_{11}$ , and  $\text{Li}_6\text{Eu}_5\text{Sn}_9$ , contain exactly the same columns of eclipsed  $\text{Sn}_5^{6-}$  aromatic rings separated by Ae or Re cations (Figure 1) as in  $\text{Na}_8(\text{Ba}/\text{Eu})\text{Sn}_6$ . Apparently, these columns are very stable formations in the presence of Ae/Re cations in such highly reduced systems and appear to be the guiding structural motif in the structure formation. It seems the primary driving force for the formation of these four different structures is the formation of the columns and their packing into bundles. The four different structures have different overall numbers of positive charges and different fractions of alkaline- or rare-earth cations, and these factors define different secondary motifs that pack with the columns. Thus, as mentioned above, the secondary motif in the reported  $\text{Na}_8(\text{Ae}/\text{Re})\text{Sn}_6$  is an isolated tin atom.<sup>13</sup> In addition to the columns,  $\text{Li}_{9-x}(\text{Eu}/\text{Ca})\text{Sn}_{6+x}$  contains bent tin trimers and isolated tin atoms while the more reduced  $\text{Li}_5\text{Ca}_7\text{Sn}_{11}$  and  $\text{Li}_6\text{Eu}_5\text{Sn}_9$  exhibit flat zigzag hexamers and infinite flat zigzag chains, respectively. The columns of pentagonal rings disappear in the most reduced compounds of this series, namely  $\text{LiMg}(\text{Eu}/\text{Sr})_2\text{Sn}_3$  which contain only flat zigzag infinite chains and isolated tin atoms. Similar hexamers and flat zigzag chains have been observed for silicon before.<sup>20,21</sup>

The distances in the pentagons of  $\text{Sn}_5^{6-}$  (Figure 2) vary somewhat from compound to compound but are all shorter than the single-bond distances of 3.067(2)–3.167(3) Å observed in  $\text{Ca}_{31}\text{Sn}_{20}$  but longer than 2.865(2) Å observed for  $[\text{Sn}=\text{Sn}]^{4-}$  in  $\text{Li}_{13}\text{Sn}_5$ .<sup>22,23</sup> The bonding and the electronic structure of the pentagon can be derived from its analogy with the cyclopentadienyl anion,  $\text{C}_5\text{H}_5^-$ , where the pairs of bonding electrons of the C–H bonds are replaced with lone

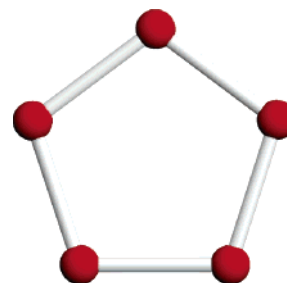


**Figure 2.** Aromatic  $\text{Sn}_5^{6-}$  in  $\text{Li}_{9-x}\text{EuSn}_{6+x}$ ,  $\text{Li}_{9-x}\text{CaSn}_{6+x}$ ,  $\text{Li}_5\text{Ca}_7\text{Sn}_{11}$ , and  $\text{Li}_6\text{Eu}_5\text{Sn}_9$  with average Sn–Sn distances of 2.924, 2.920, 2.899, and 2.911 Å, respectively. For comparison, the average distance in  $\text{Na}_8\text{EuSn}_6$  is 2.883 Å. The rings in all five compounds are perfectly flat with angles adding to exactly 540°.

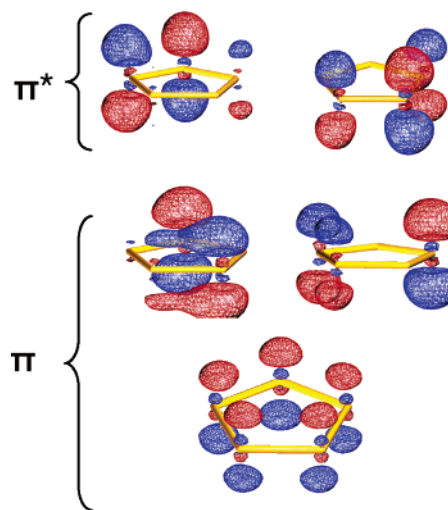


**Figure 3.** Three  $\pi$ -bonding and two  $\pi$ -antibonding molecular orbitals in the aromatic  $\text{Sn}_5^{6-}$  derived from single-point DFT calculations. These clearly resemble the  $\pi$ -manifold in the aromatic cyclopentadienyl anion,  $\text{C}_5\text{H}_5^-$ .

pairs of electrons at each tin atom. Another view of the species is to consider it as an *arachno*-cluster derived from *closo*- $\text{Sn}_7^{2-}$  with the shape of pentagonal bipyramid where the two apical atoms are removed. The number of required delocalized cluster-bonding electrons is preserved, i.e., 16, and the removal of the two apical tin positions that contribute two electrons each leads to increase of the charge to 6–, i.e.,  $\text{Sn}_5^{6-}$ . The three-dimensional delocalization of bonding electrons in *closo*- $\text{Sn}_7^{2-}$  is reduced to two-dimensional delocalization in  $\text{Sn}_5^{6-}$ , a phenomenon commonly known as aromaticity. Calculations performed on one of these rings clearly show the typical three filled  $\pi$ -bonding and two empty  $\pi$ -antibonding orbitals defining a HOMO–LUMO gap of about 2.25 eV for  $\text{Sn}_5^{6-}$  (Figure 3).

**$\text{Li}_{9-x}(\text{Eu}/\text{Ca})\text{Sn}_{6+x}$ .** In addition to the columns of pentagonal rings, the structure of  $\text{Li}_{9-x}(\text{Eu}/\text{Ca})\text{Sn}_{6+x}$  contains two additional tin sites which, if fully occupied, would form a zigzag chain. However, one of the sites refines with partial tin occupancy, and is most likely taken by lithium when available. This partial occupancy means that the would be zigzag “chain” is broken into smaller pieces, most likely bent trimers and isolated tin atoms,  $\text{Sn}^{4-}$ , in close to equal proportions (Figure 4). The distances in the trimers are about 3.16 Å and, therefore, should be considered as single bonds.

(20) Wengert, S.; Nesper, R. *Z. Anorg. Allg. Chem.* **1998**, *624*, 1801.

(21) Wengert, S.; Nesper, R. *Inorg. Chem.* **2000**, *39*, 2861.

(22) Ganguli, A. K.; Guloy, A. M.; Escamilla, A.; Corbett, J. D. *Inorg. Chem.* **1993**, *32*, 4349.

(23) Frank, U.; Muller, W. *Z. Naturforsch.* **1975**, *30b*, 316.

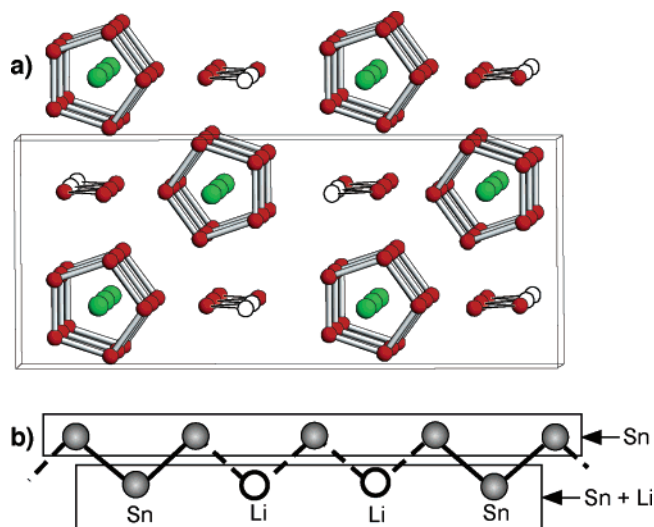


**Figure 4.** (a) General view of the structure of  $\text{Li}_{9-x}(\text{Eu}/\text{Ca})\text{Sn}_{6+x}$  along the  $a$  axis ( $b$  is horizontal, Li is omitted for clarity, Eu/Ca in green). The zigzag chains that pack with the columns of pentagonal rings are made of two sites; one is fully occupied by tin but the second one is with mixed Sn and Li occupancy. (b) Closer view of the would-be zigzag chain that breaks into bent trimers and isolated tin atoms,  $\text{Sn}_3^{8-}$  and  $\text{Sn}^{4-}$ , respectively.

Following the octet rule, the two terminal tin atoms are formally  $\text{Sn}^{3-}$  because of the one single bond to each of them while the middle tin atom is two-bonded and therefore  $\text{Sn}^{2-}$ . The overall charge of the trimer becomes 8-, i.e.,  $\text{Sn}_3^{8-}$ . The formula of the compound multiplied by three is close to  $\text{Li}_{\sim 26}(\text{Eu}/\text{Ca})_3\text{Sn}_{\sim 19}$  and can be rationalized as  $26\text{Li}^+ + 3(\text{Eu}/\text{Ca})^{2+} + 3\text{Sn}_5^{6-} + \text{Sn}_3^{8-} + \text{Sn}^{4-}$ . This means that there are approximately two extra electrons available from the cations. The existence of extra electrons is consistent with the results from the conductivity measurements which indicate that both the Ca and Eu compounds are metallic. This means that the extra electrons are delocalized over the whole structure, presumably on overlapping cationic  $s$ -orbitals and the lowest lying antibonding orbitals of the anions. The latter are most likely the  $\pi^*$  orbitals of  $\text{Sn}_5^{6-}$  because the available empty levels of the isolated  $\text{Sn}^{4-}$  are from the next electronic shell of the atoms while those for  $\text{Sn}_3^{8-}$  are of  $\sigma^*$  type, both expected to be at higher energies. The  $s$ -orbitals of Ca and Eu are of lower energies compared to lithium and, among the cations, are expected to carry most of the delocalized electrons. Furthermore, the positioning of Ca and Eu between the rings provides for good overlap between their  $s$ -orbitals and the  $\pi^*$  orbitals of  $\text{Sn}_5^{6-}$  (Figure 3). The nonzero population of the  $\pi^*$  may be the reason for the slightly longer Sn–Sn average distance of  $\text{Sn}_5^{6-}$  in  $\text{Li}_{9-x}\text{EuSn}_{6+x}$  and  $\text{Li}_{9-x}\text{CaSn}_{6+x}$ , 2.924 and 2.920 Å, respectively, compared to that distance in the electronically balanced and semiconducting  $\text{Na}_8\text{EuSn}_6$ , 2.883 Å.<sup>13</sup>

**$\text{Li}_5\text{Ca}_7\text{Sn}_{11}$ .** The “secondary” motif in the more reduced  $\text{Li}_5\text{Ca}_7\text{Sn}_{11}$  is a flat oligomer of six tin atoms. These hexamers are stacked in an eclipsed manner on top of each other and form columns parallel to those of the pentagonal rings (Figure 5). Furthermore, similarly to the latter, the hexamers are also separated by alkaline-earth cations within the columns, two such cations between each pair. The cations are positioned above and below the two loops of the hexamer and are

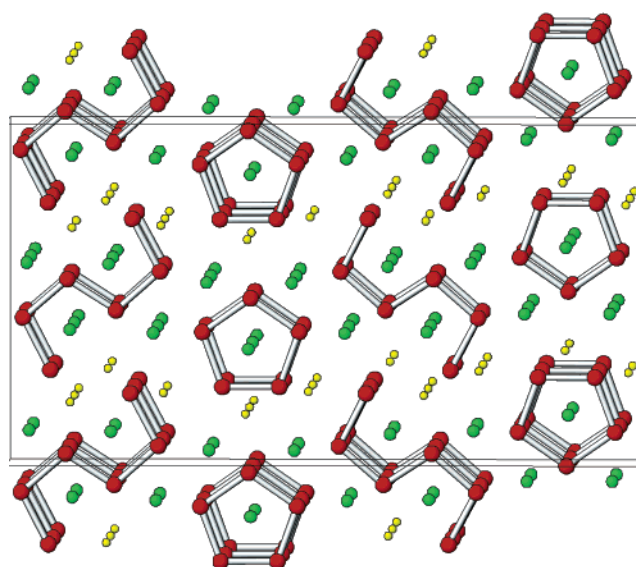


**Figure 5.** View of the structure of  $\text{Li}_5\text{Ca}_7\text{Sn}_{11}$  along the  $a$ -axis ( $c$  is horizontal; Li, yellow; Ca, green). Flat zigzag hexamers of tin are stacked on top of each other to form columns along  $a$  that are parallel to the columns of stacked pentagonal rings of tin. Both the rings and the hexamers alternate with calcium cations within the columns.

coordinated by eight tin atoms each, four from each hexamer above and below. A closer look at the hexamer and its surroundings reveals that there are two lithium cations in the plane of the hexamer that, when connected to the nearby tin atoms, complete the hexamer to a formation of two fused pentagons as shown in Figure 6. In light of this view, each calcium cation is between two eclipsed “ $\text{LiSn}_4$ ” pentagons exactly in the same way as the calcium cations in the columns of tin-only pentagons.

The distances in the hexamer, 2.948(1) Å at the ends, 2.927(1) Å next to them, and 2.859(1) Å in the middle, are also shorter than single-bond distances. Especially short is the central distance and suggests double-bond character, i.e.,  $\text{Sn}^3-\text{Sn}=\text{Sn}-\text{Sn}-\text{Sn}^2-\text{Sn}^3$  and results in a charge of 12- for the whole hexamer, i.e.,  $\text{Sn}_6^{12-}$ . The double bond in the middle, the planarity of the hexamer, and the relatively short remaining distances suggest that  $\pi$ -delocalization may be taking place. Single-point DFT calculations indicate a large HOMO–LUMO gap for  $\text{Sn}_6^{12-}$  (ca. 1.25 eV) confirming the assignment of the formal charge. Furthermore, one of the filled molecular orbitals, HOMO-5, is clearly  $\pi$ -bonding in the middle while the LUMO is the corresponding  $\pi$ -antibonding molecular orbital (see the Supporting Information). More detailed calculations performed on a similar hexamer of silicon have shown that the double bond is delocalized over the internal four atoms of the hexamer as in a conjugated system, and this delocalization keeps it flat.<sup>21</sup> Furthermore, the two lithium cations in  $[\text{Li}_2\text{Sn}_6]$  that complete the hexamer to two fused pentagons most likely help in keeping the structure planar. The silicon hexamer does not have such cations nearby and, as a result, the loops are significantly more open. With the two lithium cations included, the two fused pentagons will have a formal charge of 10-, i.e.,  $[\text{Li}_2\text{Sn}_6]^{10-}$ ,

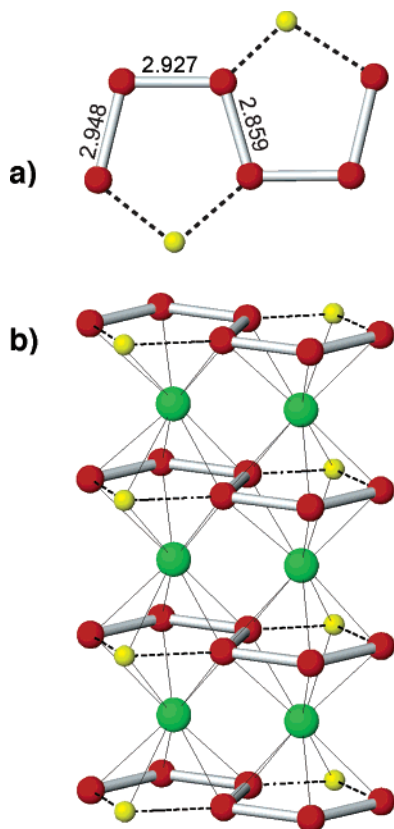


**Figure 6.** (a) Close view of the flat hexamer in  $\text{Li}_5\text{Ca}_7\text{Sn}_{11}$  (Sn–Sn distances are shown) with lines drawn to nearby coplanar lithium cations. The latter complete the hexamer to two fused pentagons. (b) Fused pentagons of  $[\text{Li}_2\text{Sn}_6]$  are stacked on top of each other with two  $\text{Ca}^{2+}$  cations between each pair forming double columns.

and are isoelectronic with the aromatic dianion  $\text{C}_8\text{H}_6^{2-}$  (10  $\pi$ -electrons) made of two fused cyclopentadienyl rings. It is assumed that the two lithium apexes in  $[\text{Li}_2\text{Sn}_6]^{10-}$  do not carry lone pairs. Instead, they interact with the lone pairs of two other nearby tin atoms that complete their coordination to tetrahedral. Similar role for lithium is observed in  $\text{Rb}_4\text{-Li}_2\text{Sn}_8$  where two lithium cations cap the square faces of a square antiprism of *arachno*- $\text{Sn}_8^{6-}$  completing it to a classical *closo*- $[\text{Li}_2\text{Sn}_8]^{4-}$  with the shape of a bicapped square antiprism.<sup>10</sup> Furthermore, as in  $[\text{Li}_2\text{Sn}_6]^{10-}$ , instead of carrying lone pairs, the lithium cations interact with the lone pairs of two nearby tin atoms from another cluster. Such substantially more covalent interactions of lithium with main-group elements have been discussed in more detail elsewhere.<sup>9,10</sup>

$\text{Li}_5\text{Ca}_7\text{Sn}_{11}$  contains one pentagonal ring of  $\text{Sn}_5^{6-}$  and one hexamer of  $\text{Sn}_6^{12-}$  per formula unit, and this means that there is an extra electron provided by the five  $\text{Li}^+$  and seven  $\text{Ca}^{2+}$  cations; i.e., the formula can be written as  $(\text{Li}^+)_5(\text{Ca}^{2+})_7(\text{Sn}_5^{6-})(\text{Sn}_6^{12-}) + e^-$ . The magnetic and conductivity measurements carried out on the compound are in agreement with this assignment. They show temperature-independent positive magnetic susceptibility and metallic conductivity, respectively. As in  $\text{Li}_{9-x}(\text{Eu}/\text{Ca})\text{Sn}_{6+x}$ , the extra electron is most likely delocalized over  $\pi$ -antibonding tin orbitals and calcium *s*-orbitals. In addition to the  $\pi^*$  orbitals of the tin pentagons and the *s*-orbitals of the calcium cations between them, available in this compound are also the  $\pi^*$  orbitals of the

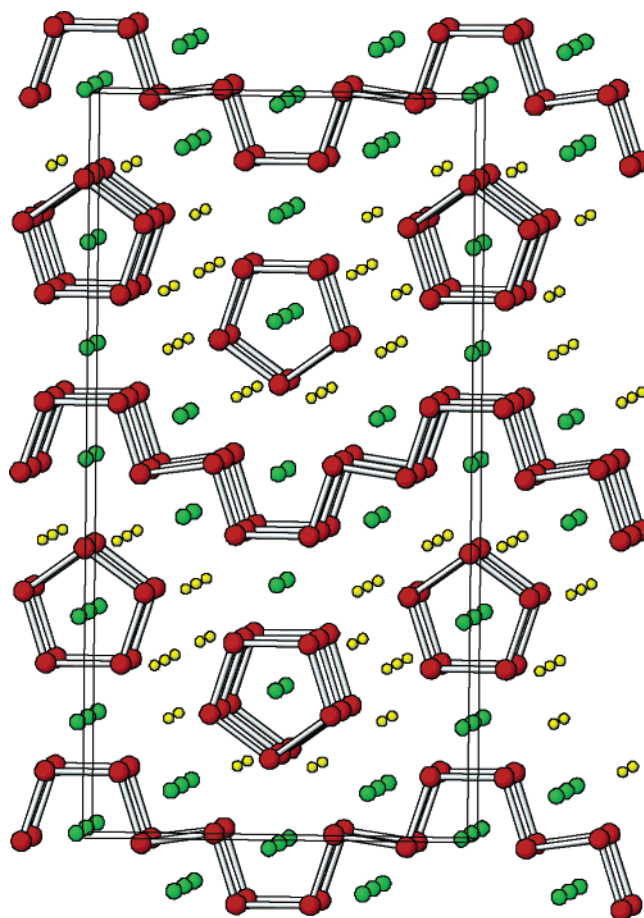


**Figure 7.** General view of the structure of  $\text{Li}_6\text{Eu}_5\text{Sn}_9$  along the *a*-axis (*b* is horizontal; Li, yellow; Eu, green). In addition to the columns of stacked pentagons along *a*, there are infinite and flat zigzag chains along *b*. The chains are stacked on top of each other along *a* and are separated by Eu cations.

$\text{Sn}_6^{12-}$  hexamers and the corresponding calcium cations that separate them (Figure 6). Therefore, it is most likely that the delocalization of the extra electron is within both types of columns. Again, the average distance within  $\text{Sn}_5^{6-}$  in  $\text{Li}_5\text{-Ca}_7\text{Sn}_{11}$ , 2.899 Å, is somewhat longer than that in the electronically balanced  $\text{Na}_8\text{EuSn}_6$ , 2.883 Å.<sup>13</sup> Despite this longer average distance, one of the distances in the pentagons in  $\text{Li}_5\text{Ca}_7\text{Sn}_{11}$  is quite short, 2.828(1) Å, and suggests some degree of localization of the  $\pi$ -bonding, perhaps close to a pentagon with one double bond, i.e., cyclopentene-like  $\text{Sn}_5^{8-}$ .

**$\text{Li}_6\text{Eu}_5\text{Sn}_9$ .** Moving to the more tin-reduced compound  $\text{Li}_6\text{-Eu}_5\text{Sn}_9$ , in addition to the primary columns of stacked pentagonal rings, we find flat zigzag chains as the secondary motif (Figure 7). The chains run perpendicular to the columns but are stacked eclipsed to each other along the same direction as the columns. Like the pentagons and the hexamers in  $\text{Li}_5\text{Ca}_7\text{Sn}_{11}$ , the chains are separated also by the divalent cations, Eu in this case. These cations are positioned above and below every bend in the chain in such a way that each Sn–Sn bond is coordinated by four such cations, two above and two below. The same type of a chain has been observed for silicon in  $\text{SrLaSi}_2$ , and each Si–Si bond is similarly coordinated by four cationic positions with mixed

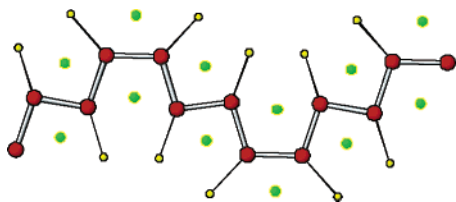


**Figure 8.** Fragment of the flat zigzag chain in  $\text{Li}_6\text{Eu}_5\text{Sn}_9$  with lines drawn to nearby coplanar lithium cations. The resulting chain of  $(\text{LiSn})_\infty$  resembles a chain of polyacetylene,  $(\text{CH})_\infty$ , where the role of hydrogen is played by lithium. The light-green spheres are europium cations above and below the plane of the chain.

Sr/La content.<sup>24</sup> The difference in the tin chain is that each tin atom, exactly as in the hexamers of the previous compound, has one nearby lithium cation in the plane of the chain (Sn–Li: 2.772(9) and 2.856(9) Å). Clearly, the lithium cations interact with the lone pairs of the formally  $\text{sp}^2$  tin atoms as described for the hexamers. When these Sn–Li interactions are drawn, as shown in Figure 8, the chain of  $(\text{SnLi})_\infty$  becomes more familiar looking. It clearly resembles polyacetylene  $(\text{CH})_\infty$  where the role of the hydrogen atoms is played by lithium (Figure 8). Also, as could be expected for doped polyacetylene, the cations, Eu in this case, are coordinated to the conjugated  $\pi$ -system by encompassing the Sn–Sn bonds (Figure 8).

The distances in the chain are quite short, 2.867(1), 2.878(1), and 2.890(1) Å, and support a conjugated model for the  $\pi$ -system. They are actually shorter than the distances in the pentagons of this compound, an average of 2.911 Å. The bond order calculated with Pauling's formula yields a value of 1.489, very close to the ideal of 1.5.<sup>25</sup> One extreme model for the chain is to assume  $\text{sp}^2$ -type tin atoms with alternating double and single bonds as in polyacetylene. This would result in a formal charge of 1– per tin atom and 6 extra electrons per formula, i.e.,  $\text{Li}_6\text{Eu}_5\text{Sn}_9 = (\text{Li}^+)_6(\text{Eu}^{2+})_5(\text{Sn}_5^{6-}) - (\infty[\text{Sn}_4^{4-}]) + 6e^-$ . The other extreme is formal  $\text{sp}^3$  hybridization for the tin atoms and a formal charge of 2– per atom. This, however, still results in extra electrons, i.e.,  $\text{Li}_6\text{Eu}_5\text{Sn}_9 = (\text{Li}^+)_6(\text{Eu}^{2+})_5(\text{Sn}_5^{6-})(\infty[\text{Sn}_4^{8-}]) + 2e^-$ . The density of states (DOS) for the chain calculated by the extended-Hückel approach showed, as expected, a partially filled band for  $\infty[\text{Sn}^-]$  and completely filled band for  $\infty[\text{Sn}^{2-}]$ . Also as expected, the Sn–Sn COOP curve is  $\pi$ -antibonding above the Fermi level for  $\infty[\text{Sn}^-]$ . Therefore, the formal charge of tin in the chains is somewhere between 2– and 1–. This means that the number of extra electrons is anywhere between 2 and 6. The observed metallic conductivity by four-probe conductivity measurements is in agreement with this assignment. It should be pointed out that the same excess of electrons is observed for the silicon chains in  $\text{SrLaSi}_2$  where assignments of  $\infty[\text{Si}^{2-}]$  or  $\infty[\text{Si}^-]$  results similarly in 2 and 6 extra electrons per 4 silicon atoms, respectively, i.e.,  $(\text{Sr}^{2+})_2(\text{La}^{3+})_2(\infty[\text{Si}_4^{8-}]) + 2e^-$  and  $(\text{Sr}^{2+})_2(\text{La}^{3+})_2(\infty[\text{Si}_4^{4-}]) + 6e^-$ .<sup>24</sup> The extra electrons in both compounds are evidently delocalized over the structures. However, in addition to the  $\pi^*$ -band in  $\text{SrLaSi}_2$ , they must either partially populate  $\sigma^*$

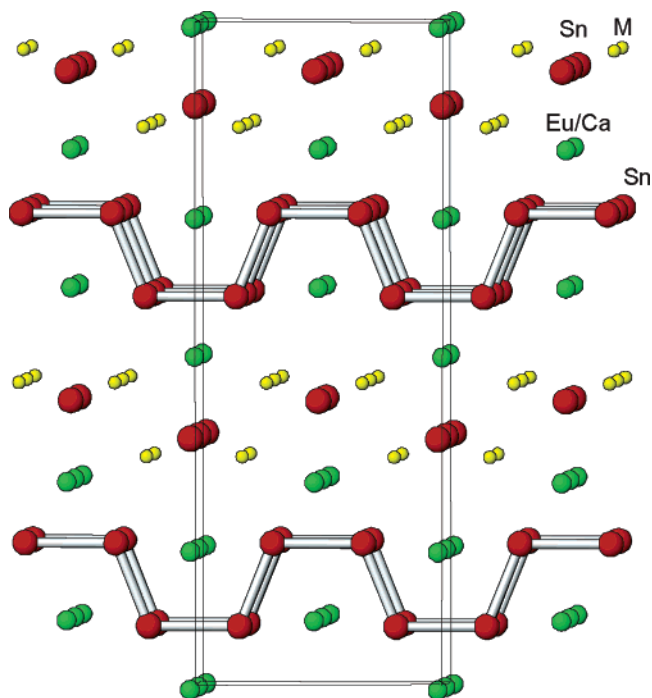


**Figure 9.** General view of the structure of  $\text{LiMg}(\text{Eu}/\text{Sr})_2\text{Sn}_3$  along the  $a$ -axis ( $c$  is horizontal,  $M = \text{Li} + \text{Mg}$  mixed position) with flat zigzag chains and isolated atoms of tin. The chains are stacked on top of each other along  $a$  and are separated by Eu or Sr cations.

of the chains or be delocalized only over the cations. On the other hand, because  $\text{Li}_6\text{Eu}_5\text{Sn}_9$  also contains pentagons of  $\text{Sn}_5^{6-}$ , these additional electrons can also populate partially the  $\pi^*$  of the pentagons. One indication for partially populated  $\sigma^*$  of the chains in  $\text{SrLaSi}_2$  and the lack of such in  $\text{Li}_6\text{Eu}_5\text{Sn}_9$  can be found in the distances in the chains of the two compounds. While the Si–Si distances are relatively long in the silicon chains, 2.447(5), 2.497(3), and 2.506(5) Å, the Sn–Sn distances in the tin chains are relatively short, 2.867(1), 2.878(1), and 2.890(1) Å. Also, the average distance in the  $\text{Sn}_5^{6-}$  pentagons of  $\text{Li}_6\text{Eu}_5\text{Sn}_9$ , 2.911 Å, is again longer than that in the electronically balanced  $\text{Na}_5\text{EuSn}_6$ , 2.883 Å, and agrees with partial population of  $\pi^*$  of the former.

**$\text{LiMg}(\text{Eu}/\text{Sr})_2\text{Sn}_3$ .** Formally, the tin atoms in these two isostructural compounds are the most reduced among all reported here. The compounds represent the only structure without pentagonal rings. Their structure contains single tin atoms and flat zigzag chains similar to those of  $\text{Li}_6\text{Eu}_5\text{Sn}_9$  but with a different *cis* and *trans* sequence (Figure 9). Like the chains in  $\text{Li}_6\text{Eu}_5\text{Sn}_9$ , the latter are also stacked eclipsed on top of each other. The Eu and Sr cations separate the chains and are coordinated around the Sn–Sn bonds with two above and two below each bond, as in  $\text{Li}_6\text{Eu}_5\text{Sn}_9$ . The distances in these chains, 2.793(2) and 2.833(2) Å in the Eu compound and 2.779(2) and 2.822(2) Å in the Sr analogue, are very short, shorter even than the already short distances in the chains of  $\text{Li}_6\text{Eu}_5\text{Sn}_9$ . Similar silicon chains with similarly short distances, 2.366 and 2.408 Å, are reported in  $\text{BaMg}_{0.1}\text{Li}_{0.9}\text{Si}_2$ .<sup>21</sup> Each bond in these chains is coordinated by two  $\text{Ba}^{2+}$  and two mixed  $[0.9(\text{Li}) + 0.1(\text{Mg})]$  positions. The latter two cations are found mixed in  $\text{LiMg}(\text{Eu}/\text{Sr})_2\text{Sn}_3$

(24) Leoni, S. Ph.D. Thesis, ETH Zurich, 1999.

(25) Pauling, L. *The Nature of the Chemical Bond*, 3rd ed.; Cornell University Press: New York, 1960; p 239.

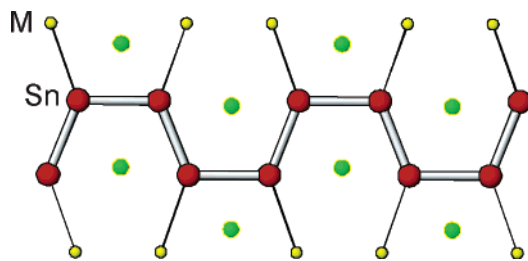


**Figure 10.** Fragment of the flat zigzag chain in  $\text{LiMg}(\text{Eu/Sr})_2\text{Sn}_3$  with lines drawn to nearby coplanar M positions of mixed Li + Mg occupancy. The resulting chain resembles a chain of polyacetylene,  $(\text{CH})_\infty$ . The light-green spheres are Eu or Sr cations above and below the plane of the chain.

as well. However, the mixed positions (M) contain almost equal amounts of Li and Mg and play quite a different role in the tin compound. They are in the planes of the chains and each is very close to one tin atom (Figure 10), exactly like the lithium cations in the chains of  $\text{Li}_6\text{Eu}_5\text{Sn}_9$ . Again, their positioning resembles that of hydrogen in polyacetylene and indicates substantial covalent (Li/Mg)–Sn interactions.

Assuming complete charge transfer from the cations and a polyacetylene-like conjugated  $\pi$ -system of alternating single and double bonds along the Sn–Sn chain ( $\text{Sn}^-$ ), the formula of  $\text{LiMg}(\text{Eu/Sr})_2\text{Sn}_3$  can be written as  $(\text{Li}^+)(\text{Mg}^{2+})-(\text{Eu/Ca})^{2+}_2(\text{Sn}^{4-})_\infty[\text{Sn}_2^{2-}] + e^-$ . This means that there are 0.5 extra electrons per  $\text{Sn}^-$  of the chain in this compound instead of the 1.25 such electrons per  $\text{Sn}^-$  in the chain of  $\text{Li}_6\text{Eu}_5\text{Sn}_9$ . Therefore, fewer electrons are expected to populate the  $\pi$ -antibonding levels in the chains of  $\text{LiMg}(\text{Eu/Sr})_2\text{Sn}_3$  and this may explain the observed shorter Sn–Sn distances compared to those in  $\text{Li}_6\text{Eu}_5\text{Sn}_9$ . The extra electrons are again delocalized over the whole structure (partially filled band in DOS) and both the Eu and Sr compounds show metallic conductivity. Alternatively, the extra electron may be delocalized only on the chains and not on cations, i.e.,  $[\text{Sn}_2^{3-}]_\infty$ . This would make the chains isoelectronic (and isostructural) with the S–N chains of polythiazyl  $[\text{SN}]_\infty$ .<sup>26</sup> The three  $\pi$  electrons per repeating unit in the latter make it metallic as well.

**Magnetic Properties.** The three Eu-containing compounds are paramagnetic with  $\mu_{\text{eff}}$  of ca. 7.85, 17.68, and 10.26  $\mu_B$  for  $\text{Li}_{9-x}\text{EuSn}_{6+x}$ ,  $\text{Li}_6\text{Eu}_5\text{Sn}_9$ , and  $\text{LiMgEu}_2\text{Sn}_3$ , respectively. These values are in good agreement with the expected spin-only moments of 7.94, 17.75, and 11.22  $\mu_B$  for one, five, and two Eu(II) cations, respectively.  $\text{Li}_{9-x}\text{EuSn}_{6+x}$ ,  $\text{Li}_6\text{Eu}_5\text{Sn}_9$ , and the previously reported  $\text{Na}_8\text{EuSn}_6$  show magnetic transitions at low temperatures (Figures in Supporting Information) while  $\text{LiMgEu}_2\text{Sn}_3$  does not show such transitions. Note that the first three compounds contain columns of stacked pentagons (with Eu cations between the pentagons) while  $\text{LiMgEu}_2\text{Sn}_3$  does not contain such columns. The transitions for  $\text{Li}_{9-x}\text{EuSn}_{6+x}$  occur at ca. 10 and 21 K and seem to be both antiferromagnetic (similar traces in ZFC and FC modes).  $\text{Li}_6\text{Eu}_5\text{Sn}_9$  also shows two transitions, at ca. 8 and 30 K, but while the latter is antiferromagnetic, the former is ferromagnetic, i.e., the magnetization in ZFC mode

is lower than that in FC mode below 8 K and decreases with lowering the temperature. As already reported,  $\text{Na}_8\text{EuSn}_6$  shows also two magnetic transitions, both antiferromagnetic and at ca. 20 and 70 K. This compound as well as  $\text{Li}_{9-x}\text{EuSn}_{6+x}$  have only one type of magnetic center, the Eu(II) cations that separate the stacked pentagonal rings in the columns. Furthermore, these magnetic centers are quite far apart, more than 4.8 Å, and yet both compounds show magnetic ordering. While  $\text{Li}_{9-x}\text{EuSn}_{6+x}$  is metallic and the available delocalized electrons may provide the means for magnetic communication between the localized spins (along the RKKY theory),<sup>27</sup>  $\text{Na}_8\text{EuSn}_6$  is semiconducting and the interactions between the Eu(II) cations must be via the  $\pi$ -systems of the  $\text{Sn}_5^{6-}$  pentagons. The fact that all compounds with columns of such pentagons show magnetic transitions suggests that this type of interactions, i.e., between the  $\pi^*$  orbitals of the rings and the  $s$ -orbitals of the dications, may be relatively strong and predominant even when conducting electrons are available. As discussed above, the extra electrons are most likely delocalized over the Eu(II) cations and the  $\pi^*$  systems of the pentagons.

It is very difficult to establish the nature of the magnetic transitions in these compounds based solely on magnetic measurements. Careful and extensive neutron diffraction experiments at different temperatures are necessary for this. Unfortunately, all these compounds are highly air- and moisture-sensitive and their handling and transportation to neutron sources makes this endeavor extremely difficult and time-consuming.

## Summary

The six new compounds of four different structural types described here,  $\text{Li}_{9-x}\text{CaSn}_{6+x}$ ,  $\text{Li}_{9-x}\text{EuSn}_{6+x}$ ,  $\text{Li}_5\text{Ca}_7\text{Sn}_{11}$ ,  $\text{Li}_6\text{Eu}_5\text{Sn}_9$ ,  $\text{LiMgEu}_2\text{Sn}_3$ , and  $\text{LiMgSr}_2\text{Sn}_3$ , together with three previously reported isostructural compounds,  $\text{Na}_8\text{BaSn}_6$ ,  $\text{Na}_8\text{BaPb}_6$ , and  $\text{Na}_8\text{EuSn}_6$ , form a new class of compounds with heavy metal aromatic or conjugated systems. The number of these compounds with such heavy metals is already respectful and is a good indication for more to be expected. Most extraordinary in these compounds is the existence of one and the same structural feature for most of them, columns of stacked pentagonal rings of  $\text{Sn}_5^{6-}$  (or  $\text{Pb}_5^{6-}$ ). This indicates that aromaticity in heavy metals is not just one isolated case but occurs rather often in a variety of compounds. Furthermore,  $\pi$ -conjugation in flat oligomers and polymers seems to be similarly common. All six newly reported compounds are metallic and some of the europium-containing compounds show magnetic transitions and, therefore, qualify to be called metallic and/or magnetic Zintl phases.

**Acknowledgment.** We thank the National Science Foundation (CHE-0446131) for financial support of this research.

**Supporting Information Available:** X-ray crystallographic file in CIF format (six structures), a table with important distances and angles for the six compounds, plots of the magnetic susceptibilities

(26) Cohen, M. J.; Garito, A. G.; Heeger, A. J.; MacDiarmid, A. G.; Mikulski, C. M.; Saran, M. S.; Kleppinger, J. J. *Am. Chem. Soc.* **1975**, *98*, 3844.

(27) Kittel, C. *Solid State Phys.* **1968**, *22*, 1.

***Heavy-Metal Aromatic and Conjugated Species***

vs temperature for  $\text{Li}_{9-x}\text{EuSn}_{6+x}$  and  $\text{Li}_6\text{Eu}_3\text{Sn}_9$  measured in FC and ZFC modes at low temperatures, the same plots at high temperatures with their Curie–Weiss fits, a picture of the  $\pi$ -orbitals of the hexamer in  $\text{Li}_5\text{Ca}_7\text{Sn}_{11}$  calculated from DFT, and complete

ref 17. This material is available free of charge via the Internet at <http://pubs.acs.org>.

IC050803T